The Astrophysical Journal, 585:191–204, 2003 March 1

GALAXY CLUSTERING EVOLUTION IN THE UH8K WEAK-LENSING FIELDS[1]

Gillian Wilson[2,3]

Received 2002 August 15; accepted 2002 November 6

ABSTRACT

We present measurements of the two-point galaxy angular correlation function as a function of apparent magnitude, color, and morphology. Our analysis utilizes images taken using the UH8K CCD mosaic camera on the Canada-France-Hawaii Telescope. Six $0.^{\circ}5 \times 0.^{\circ}5$ fields were observed for a total of 2 hr each in I and V, resulting in catalogs containing ~25,000 galaxies per field. We present new galaxy number counts to limiting magnitudes of $I = 24.0$ and $V = 25.0$. We divide each passband sample into intervals of width 1 mag. Within each magnitude interval, we parameterize the angular correlation function by $A_{\omega}\theta^{-\delta}$ and find $\omega(\theta)$ to be well described by a power law of index $\delta = 0.8$. We find the amplitude of the correlation function, A_{ω}, to decrease monotonically with increasingly faint apparent magnitude. We compare with predictions that utilize redshift distributions based on deep spectroscopic observations. We conclude that simple redshift-dependent models that characterize evolution by means of the ϵ parameter inadequately describe the observations. This is because the predictions do not allow for the varying mix of morphologies and absolute luminosities (and hence clustering strengths) of galaxies sampled at different apparent magnitudes. We find a strong clustering dependence on $V-I$ color. This is because galaxies of extreme color lie at similar redshifts and the angular correlation functions for these samples are minimally diluted by chance projections. We find extremely red ($V-I = 3.0$) galaxies (likely early-type galaxies at $z \sim 1$) to have an A_{ω} about 10 times higher, and extremely blue ($V-I = 0.5$) galaxies (likely local late types) to have an A_{ω} about 15–20 times higher, than that measured for the full field population. We then present the first attempt to investigate the redshift evolution of clustering, utilizing a population of galaxies of the *same* morphological type and absolute luminosity. We study the dependence of $\omega(\theta)$ on redshift for $L*$ early-type galaxies in the redshift range $0.2 < z < 0.9$. Although uncertainties are large, we find the evolution in the clustering of these galaxies to be consistent with stable clustering [$\epsilon = 0$ for a redshift dependence of the spatial correlation function, $\xi(r)$, parameterized as $\xi(r, z) = (r/r_0)^{-\gamma}(1+z)^{-(3+\epsilon)}$]. We find $L*$ early-type galaxies to cluster slightly more strongly (physical correlation length $r_0 = 5.25 \pm 0.28\ h^{-1}$ Mpc assuming $\epsilon = 0$) than the local full field population. This is in good agreement with the correlation length measured by the 2dF Galaxy Redshift Survey for $L*$ early-type galaxies in the local universe.

Subject headings: cosmology: observations — galaxies: evolution — galaxies: photometry — large-scale structure of universe

1. INTRODUCTION

One of the most interesting and important problems in modern astronomy is that of galaxy formation and evolution. Traditionally, galaxy distributions have been quantified using correlation functions. Two principal approaches, each with its own advantages and drawbacks, have been used to measure the two-point function, which measures the excess probability over random of finding another galaxy at a separation r from a given galaxy. One option is to compute the spatial correlation function, $\xi(r)$, or its Fourier transform equivalent, $P(k)$, directly using spectroscopic redshifts. In recent years a plethora of redshift surveys culminating in the Two-degree Field Galaxy Redshift Survey (hereafter 2dFGRS) and Sloan Digital Sky Survey (hereafter SDSS) have been providing accurate pictures of the distribution of galaxies in the local universe. The spectroscopic approach, however, is limited by the technical difficulties inherent in measuring spectra for many galaxies and the infeasibility of obtaining both a very deep and very wide sample.

In order to quantify the clustering of faint galaxies beyond spectroscopic limits the angular two-point correlation function, $\omega(\theta)$, has been the approach of choice. The power of $\omega(\theta)$ as a diagnostic of the galaxy distribution lies in the simplicity of its application; one is required only to count pairs of galaxies at given angular separations and normalize the results with respect to the number of pairs expected from a random distribution. The drawback is that angular correlation function analyses must rely on accurate observations or models of the redshift distribution of faint galaxies to invert $\omega(\theta)$ and hence deduce the three-dimensional correlation length, r_0.

Pioneering studies of $\omega(\theta)$ using photographic plates were carried out by Groth & Peebles (1977), Phillipps et al. (1978), Shanks et al. (1980), Maddox et al. (1990), Bernstein et al. (1994), and Infante & Pritchet (1995), among others. In the last decade or so the widespread use of charge-coupled device (CCD) cameras have permitted studies reaching far deeper limiting magnitudes (passbands in parentheses), e.g., Efstathiou et al. (1991; U, B, R, I), Roche et al. (1993; B, R), Brainerd, Smail, & Mould (1995; R), Hudon & Lilly (1996; R), Lidman & Peterson (1996; I), Villumsen, Freudling, & da Costa (1997; R), Woods &

[1] Based on observations with the Canada-France-Hawaii Telescope, which is operated by the National Research Council of Canada, le Centre National de la Recherche Scientifique de France, and the University of Hawaii.

[2] Physics Department, Brown University, 182 Hope Street, Providence, RI 02912.

[3] SIRTF Science Center, California Institute of Technology, 220-6, Pasadena, CA 91125; gillian@ipac.caltech.edu.

Fahlman (1997; V, R, I), Brainerd & Smail (1998; I), Postman et al. (1998; I), Cabanac, de Lapparent, & Hickson (2000; V, I), Fynbo, Freudling, & Möller (2000; R, I), and McCracken et al. (2000; B, R, I, K). These investigations were able to target only one or two fields up to about 50 arcmin^2 in size. Several groups attempted to cover larger areas by mosaicking together many separate pointings (Postman et al. 1998; Roche & Eales 1999, [R]) but these observations reached much shallower limiting magnitudes. In recent years, the advent of wide-field mosaic cameras on 4 m class telescopes has begun to revolutionize the field, permitting studies of unprecedented depth and areal coverage, with the corresponding reduction in variance inherent in covering large areas of the sky (Cabanac et al. 2000; McCracken et al. 2001, [I]).

Spatial two-point correlation functions for local, bright, optically selected samples have been determined by many authors over the last few decades. Numerous studies have found $\xi(r)$ to be well described by a power law, $\xi(r) = (r/r_0)^{-\gamma}$, with slope $\gamma \simeq 1.8$ and correlation length $r_0 \simeq 5\ h^{-1}$ Mpc for $r \lesssim 15\ h^{-1}$ Mpc (Davis & Peebles 1983; Loveday et al. 1995; Norberg et al. 2001); r_0^γ may be interpreted as the correlation amplitude at $1\ h^{-1}$ Mpc. Thus the value of r_0 provides a measure of the clustering strength of galaxies in the sample, with a larger value implying stronger clustering.

In the last few years, it has become generally accepted that clustering strengths, as measured in the local universe, have a dependence on galaxy morphology (Iovino et al. 1993; Loveday et al. 1995; Hermit et al. 1996; Willmer, da Costa, & Pellegrini 1998; Norberg et al. 2002). It has been known since at least Davis & Geller (1976) that early-type galaxies (ellipticals and S0s) cluster more strongly than late types, i.e., $r_0(\mathrm{E}) > r_0(\mathrm{S})$. Estimates of the ratio of the correlation strengths $[r_0(\mathrm{E})/r_0(\mathrm{S})]^{1.8}$ for the two types range from $\sim$1.2 to $\sim$5. Claims for a luminosity dependent component to galaxy correlation strengths have been more contentious, although results from the most recent surveys (Hermit et al. 1996; Lin et al. 1996; Willmer et al. 1998; Guzzo et al. 2000; Norberg et al. 2001) do indeed seem to indicate that high-luminosity galaxies are more strongly clustered than low-luminosity galaxies. A dependence of clustering strength on both intrinsic luminosity and morphological type is to be expected if galaxies are biased tracers (see below) of the mass distribution in the universe. Early efforts to quantify galaxy evolution as a function of redshift utilizing only *one* passband proved rather limiting. This is because subsets of any given sample selected on apparent magnitude contain galaxies of differing absolute luminosities (and differing morphological types) at different redshifts, greatly complicating the analysis. Whenever two (or more) passbands have been available, color selection has often been used. Infante & Pritchet (1995), Neuschaefer & Windhorst (1995), Landy, Szalay, & Koo (1996), Roche et al. (1996), Woods & Fahlman (1997), Brown, Webster, & Boyle (2000), Cabanac et al. (2000), McCracken et al. (2001), and Zehavi et al. (2002) all found red galaxies to cluster more strongly than blue galaxies. This is most likely a manifestation of the morphological clustering dependence. A more recent innovation has been the use of multipassband data to estimate photometric redshifts (Connolly, Szalay, & Brunner 1998; Arnouts et al. 1999a; Brunner, Szalay, & Connolly 2000; Teplitz et al. 2001), a technique that bridges traditional spectroscopic and photometry camps to study galaxies in the range $0 < z \leq 1$. However, although promising, to date, photometric redshifts analyses have been limited to small fields of view.

The "ϵ" formalism, first introduced by Groth & Peebles (1977), has traditionally been used to characterize the evolution of clustering with redshift. This empirical approach assumes that the typical clustering length observed at high-redshift transitions monotonically to that observed locally. By assuming a redshift distribution and cosmology, it is possible to predict $\omega(\theta)$, compare to observations and hence determine the value of ϵ that best describes the evolution of the correlation function. Many authors have concluded, either from the aforementioned $\omega(\theta)$ studies or directly from spectroscopic studies (Le Fevre et al. 1996; Shepherd et al. 1997; Small et al. 1999; Carlberg et al. 2000; Hogg, Cohen, & Brandford 2000), that $0 < \epsilon < 2$, i.e., that galaxy clustering is either stable or grows in amplitude from $z = 1$ to the present. Undoubtedly, a lack of consistency of sample, i.e., an inability to follow the *same* population of galaxies because of changing morphological mixes and intrinsic luminosities with redshift, makes interpretation of the measurements confusing.

Strong evidence that the "ϵ" formalism might be invalid, at least at higher redshift, was provided by the discovery that clustering amplitudes measured for Lyman-break galaxies at $z \sim 3$ are similar to those measured for local galaxies (Adelberger et al. 1998; Giavalisco et al. 1998). Such strong clustering of the Lyman-break galaxies is to be expected if these galaxies are highly biased with respect to the mass distribution. In the standard hierarchical picture of galaxy formation and evolution, galaxy clustering traces overdense regions in the dark matter distribution. High-redshift galaxies are expected to form at the most extreme peaks in the density field and are thus biased tracers of the mass (Kaiser 1984; Bardeen et al. 1986). If early-type or more luminous galaxies are associated with rarer, more massive halos, then these galaxies would be expected to exhibit even stronger clustering than the galaxy population as a whole. Subsequent to the epoch of formation, the clustering of the galaxies is expected to evolve more slowly than the clustering of the dark matter so the two distributions are expected to be more similar today than in the past (Baugh et al. 1999; Kauffmann et al. 1999; Carlberg et al. 2000).

In the hierarchical formation scenario, the clustering of dark matter increases monotonically with time. The rate of evolution in the clustering of the dark matter is a function of cosmology, being faster in a high-density ($\epsilon \sim 1.0$ for $\Omega_m = 1$) than in a low-density ($\epsilon \sim 0.2$ for $\Omega_m = 0.2$) universe (Colin, Carlberg, & Couchman 1997). If the evolution in dark matter clustering could be measured directly as a function of redshift, then Ω_m, Ω_λ, and the power spectrum of density fluctuations could be inferred directly. However, in practice, one can measure only evolution in the galaxy clustering pattern. The amplitude of the galaxy correlation function is determined by a combination of factors: evolution in the underlying dark matter fluctuations plus any bias (which is also a function of cosmology) relating the galaxy overdensities to the mass. Realistically, in addition to the depth of the dark matter potential, one can expect galaxy evolution also to depend on complex physical processes involving the local environment, cooling and feedback mechanisms, and galaxy interactions. Observations of galaxy clustering at high redshift are therefore vital to constrain models of these processes empirically and deepen our

understanding of the complexities of both galaxy and structure formation and evolution.

In this paper we investigate galaxy clustering evolution on scales of up to 30′ using data collected using the University of Hawaii's 8K (UH8K) CCD mosaic camera on the Canada-France-Hawaii Telescope (CFHT). The data were obtained for a weak-lensing study of "blank fields"; i.e., the fields chosen for study were intended to be representative views of the universe not containing any unusually large masses such as rich clusters. The data are also, therefore, well suited to the study of (field) galaxy clustering and evolution.

The outline of the paper is as follows. In § 2 we describe the data and photometry. In § 3 we present both our number counts and a comparison with the counts from other groups. In § 4 we describe and discuss our measurements of the two-point correlation function as a function of median apparent magnitude, $V-I$ galaxy color, and morphological type. We compare to predictions and discuss possible sources of uncertainty. In § 5 we briefly summarize our conclusions. We assume a flat lambda ($\Omega_{m0} = 0.3, \Omega_{\lambda 0} = 0.7$) cosmology with $H_0 = 100\ h\ \mathrm{km\ s^{-1}\ Mpc^{-1}}$ throughout.

2. THE DATA AND GALAXY SAMPLES

2.1. *Data Acquisition and Reduction*

The data were taken at the 3.6 m CFHT telescope using the 8192×8192 pixel UH8K camera at prime focus. The field of view of this camera is ∼30′ with pixel size 0.″207. The data (six pointings) used in the analysis were acquired as part of an ongoing project that has the principal aim of investigating the cosmic shear pattern caused by gravitational lensing from the large-scale structure of the universe. In addition to the main project, estimates of cosmic shear variance on 2′–30′ scales (Kaiser, Wilson, & Luppino 2000), the data have also been used to investigate galaxy halos at radii of 20″–60″ (50–200 h^{-1} kpc) (Wilson et al. 2001b) and to investigate the relationship between mass and light on group and cluster scales (45″–30′) (Wilson, Kaiser, & Luppino 2001a). In this paper we focus on properties of galaxy clustering.

Table 1 gives an overview of the data, describing the field name, center, and seeing for each pointing. The reduction procedure was lengthy and involved. We defer a full description of the data reduction pipeline (involving careful registration and point-spread function correction) and the resulting catalogs to a later paper (Wilson & Kaiser 2003, in preparation). Here we provide only an overview of the photometry pipeline.

2.2. *Photometry*

The data were dark subtracted, flat-fielded, registered, median-averaged, and corrected for galactic extinction using extinction measurements from Schlegel, Finkbeiner, & Davis (1998). The UH8K science images were calibrated to the Johnson-Cousins system using a series of standard star field observations (Landolt 1992). The standard star fields were also dark subtracted and flat-fielded in a manner similar to the science frames. These were used then to calculate zero points for each pointing. In agreement with McCracken et al. (2001), our observations did not indicate the presence of a color term for either the I or V filters.

The *imcat* data reduction package[4] was used throughout. Objects were detected and assigned an optimal size by smoothing the science frames by a progressively larger series of filters as described in Kaiser, Squires, & Broadhurst (1995). Aperture magnitudes were then measured within a multiple of three times this radius.

The number counts of objects at faint magnitudes are dominated by galaxies but at brighter magnitudes the stellar component is dominant. We removed stars at brighter magnitudes ($I \lesssim 23$; $V \lesssim 24$) by hand, by means of filtering on a size-magnitude diagram. For fainter objects, no attempt was made to further eliminate stars from the sample since compact galaxies could be mistakenly removed and stellar numbers are very small relative to the galaxies at these faint limits. After stellar filtering, approximately 25,000 galaxies remained in each passband for each of the six pointings, an extremely deep and wide-area data set compared to previous studies.

3. NUMBER COUNTS

The I-band number counts (logarithm of number of galaxies degree^{-2} mag^{-1}) for each pointing are shown in Figure 1. The uncertainties shown are Poissonian. Clearly, the counts from each pointing are in good agreement with each other and are complete to $I = 24.0$. Figure 2 shows the same but for the V-band counts which are complete to $V = 25.0$.

Figure 3 compares our I number counts with those measured by other groups. Our data are shown by the filled hexagons. The measured values may be found in Table 2. The uncertainties at each magnitude were calculated from the pointing-to-pointing variations. Also shown in the figure are the counts of Postman et al. (1998), Arnouts et al.

[4] See http://www.ifa.hawaii.edu/~kaiser.

TABLE 1
FIELD CENTERS AND SEEING

Field	Pointing	RA (J2000.0)	Decl. (J2000.0)	l (deg)	b (deg)	FWHM (arcsec) I	FWHM (arcsec) V
Lockman	1	10 52 43.0	57 28 48.0	149.28	53.15	0.83	0.85
	2	10 56 43.0	58 28 48.0	147.47	52.83	0.84	0.86
Groth.....	1	14 16 46.0	52 30 12.0	96.60	60.04	0.80	0.93
	3	14 09 00.0	51 30 00.0	97.19	61.57	0.70	0.85
1650	1	16 51 49.0	34 55 02.0	57.37	38.67	0.82	0.85
	3	16 56 00.0	35 45:00.0	58.58	37.95	0.85	0.72

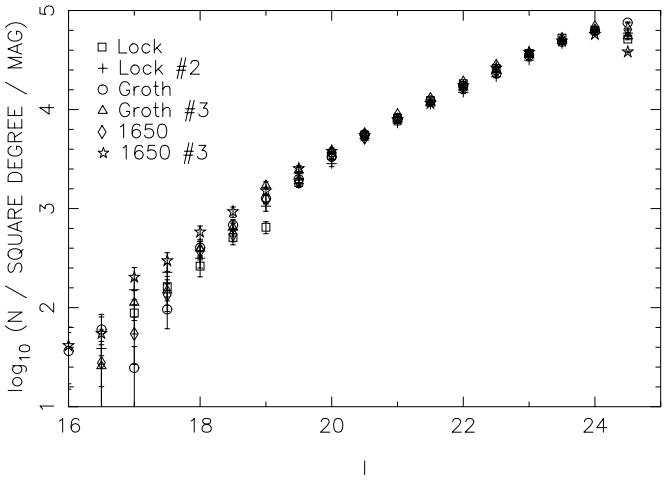

FIG. 1.—*I*-band number counts. The six pointings are as indicated by the key.

(1999b), Cabanac et al. (2000), Metcalfe et al. (2001), and McCracken et al. (2001). A correction of $I = I_{AB} - 0.43$ was applied to the counts of McCracken et al. to bring them to the Cousins *I*-band system. Clearly, the counts are in reasonably good agreement over the whole range. The highest and lowest values at each magnitude were obtained by Cabanac et al. and Postman et al., respectively. However, as discussed by Cabanac et al., that group systematically measure 20%–30% higher counts than Postman et al. but have large (0.2–0.5) errors in their zero-point calibration.

The line in Figure 3 shows the best fit (Table 3) to our counts in the range $21.0 < I < 23.5$ (slope of 0.31 ± 0.01). A comparison between our best-fit slope and the values found by other authors is shown in Table 4. Although the range over which the slope is fit varies slightly, the values are generally in good agreement.

Figure 4 shows a similar comparison, but for the (Johnson) *V* counts (note that V_{AB} = Johnson *V*). The filled hexagons in Figure 4 represent our measurements. The values are given in Table 5. *V*-band galaxy number counts are more rarely published in the literature. We compare to the counts of Gardner et al. (1996), Arnouts et al. (1999b), and Cabanac et al. (2000). We find that we are in good

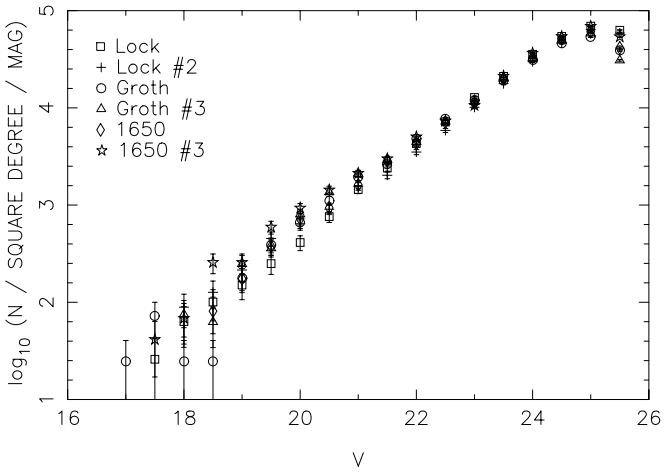

FIG. 2.—Same as Fig. 1, but for the *V* band

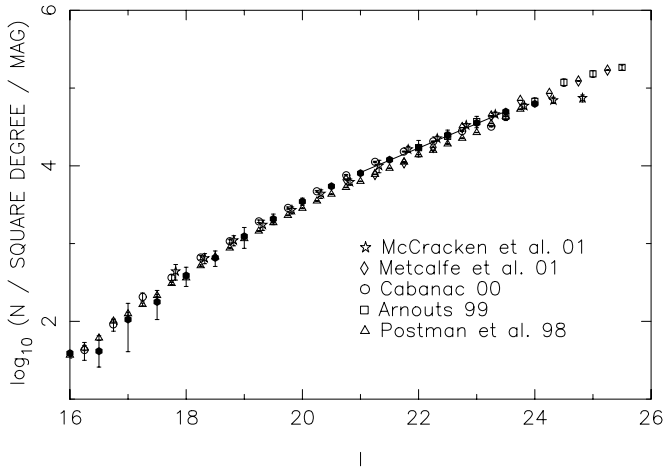

FIG. 3.—Comparison of our *I*-band number counts with measurements from other groups. The filled hexagons represent our data. The uncertainties are obtained from the pointing-to-pointing variations in Fig. 1. See Table 2 for values. The line shows the best fit to our counts in the range $21.0 < I < 23.5$ (slope of 0.31 ± 0.01).

agreement with Gardner et al. at bright magnitudes and with Arnouts et al. at faint magnitudes. However, the agreement with Cabanac et al. is rather poor. Cabanac et al., however, also report large uncertainties in their *V*-band calibration (ranging from 0.2 at bright magnitudes to 0.5 at *V* of 24).

The line in Figure 4 shows the best fit to our data in the range $22.0 < V < 24.5$ (slope of 0.43 ± 0.02). Within uncertainties, this value agrees well with the slopes reported by Woods & Fahlman (1997), Driver et al. (1994), and Smail et al. (1995) (See Table 4). Our data do not reach a sufficiently faint limit to detect any flattening of the slope reported at $V \sim 24.5$ by Smail et al.

4. THE ANGULAR CORRELATION FUNCTION

The two-point angular correlation function, $\omega(\theta)$, measures the excess probability (over a random Poisson

TABLE 2

DIFFERENTIAL COUSINS *I*-BAND COUNTS
(N deg^{-2} mag^{-1})

Magnitude	$\log_{10}(N)$	σ_{high}	σ_{low}
16.0	1.590	0.037	0.040
16.5	1.617	0.139	0.205
17.0	2.024	0.208	0.414
17.5	2.250	0.148	0.227
18.0	2.590	0.106	0.141
18.5	2.817	0.088	0.111
19.0	3.093	0.114	0.154
19.5	3.317	0.063	0.074
20.0	3.541	0.044	0.049
20.5	3.737	0.020	0.021
21.0	3.905	0.025	0.027
21.5	4.078	0.020	0.021
22.0	4.236	0.032	0.035
22.5	4.395	0.037	0.041
23.0	4.551	0.026	0.027
23.5	4.696	0.020	0.021
24.0	4.797	0.024	0.025

TABLE 3
BEST FITS TO COUNTS

Passband	Range	Slope	Intercept
I.....	[21.0–23.5]	0.31 ± 0.01	-2.68 ± 0.25
V.....	[22.0–24.5]	0.43 ± 0.02	-5.83 ± 0.45

distribution) that two galaxies will be found in the solid angle elements $d\Omega_1$ and $d\Omega_2$, separated by angle θ. It is defined by

$$dP = \bar{N}^2[1 + \omega(\theta)]\, d\Omega_1\, d\Omega_2 \,, \tag{1}$$

where dP is the joint probability of finding galaxies in the two solid angle elements, and $\bar{N}$ is the mean surface density of galaxies.

4.1. *The Dependence of $\omega(\theta)$ on Apparent Magnitude and Passband*

We compute $\omega(\theta)$ using the Landy & Szalay (1993) estimator:

$$\omega(\theta) = \frac{\mathrm{DD} - 2\mathrm{DR} + \mathrm{RR}}{\mathrm{RR}} \,, \tag{2}$$

where DD, DR, and RR are the number of data-data, data-random, and random-random pairs (scaled appropriately by the number of data and random points) at angular separations $\theta \pm d\theta$, respectively. This estimator is based on the N-point function (Szapudi & Szalay 1998) and has been shown to have the advantage of reduced edge effects and smallest possible variance.

To determine DR and RR, we generated a catalog for each pointing containing 50,000 random points covering a similar area to the data. We masked this random catalog with the same masks we used to mask out saturated stars and subquality regions of the CCDs. The remaining catalogs contained ~30,000 randomly distributed points.

We also applied an integral constraint (IC) correction (Groth & Peebles 1977). Estimating the mean galaxy density and the two-point correlation function from any survey limited in area results in a $\omega(\theta)$ artificially reduced by the amount

$$C = \frac{1}{\Omega^2} \int\int \omega(\theta)\, d\Omega_1\, d\Omega_2 \,, \tag{3}$$

TABLE 4
COMPARISON OF NUMBER COUNT SLOPES

Passband	Range	Slope	Source
I.....	[21.0–23.5]	0.31 ± 0.01	1
I.....	[20.0–24.0]	0.35 ± 0.02	2
I.....	[21.0–25.0]	0.33	3
I.....	[22.5–25.5]	0.31 ± 0.02	4
I.....	[19.0–22.5]	0.34 ± 0.03	5
V.....	[22.0–24.5]	0.43 ± 0.02	1
V.....	[22.0–24.5]	0.43 ± 0.03	6
V.....	[22.0–24.5]	0.404 ± 0.015	7
V.....	[20.5–23.0]	0.41 ± 0.01	5

REFERENCES.—(1) This work; (2) McCracken et al. 2001; (3) Metcalfe et al. 2001; (4) Arnouts et al. 1999b; (5) Driver et al. 1994; (6) Woods & Fahlman 1997 (averaged); (7) Smail et al. 1995.

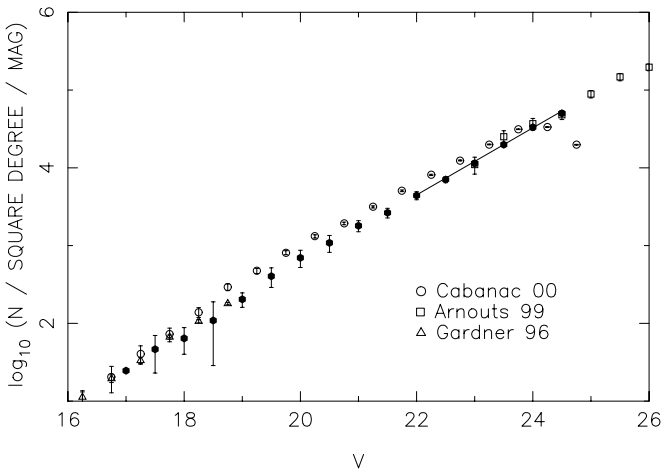

FIG. 4.—Same as Fig. 3, but for V counts. See Table 5 for values. The line shows the best fit to our counts in the range $22.0 < V < 24.5$ (slope of 0.43 ± 0.02).

where the integrals are performed over the total solid angle, Ω, subtended by each of the pointings after masking by the detection masks (Roche & Eales 1999). The correction is a function of the effective survey area and, to a lesser extent, the survey geometry. Because the mean density measured from a large CCD more closely approximates that of the mean global value, the correction is smaller for larger fields of view.

In practice $\omega(\theta)$ is calculated without the correction, equation (3) is integrated over all elements of solid angle $d\Omega_i$ in the survey area and then $\omega(\theta)$ is recalculated with the correction added. A stable solution is reached by iteration. In order to calculate the correction it is therefore necessary to assume a functional form for the two-point correlation function. For local, bright, optically selected galaxy samples $\omega(\theta)$ has been shown to be well approximated by a power law,

$$\omega(\theta) = A_w \theta^{-\delta} \,, \tag{4}$$

with $\delta = 0.8$ and where A_ω is the amplitude of $\omega(\theta)$. [Measuring angular separation in arcminutes as we do here, A_ω is then defined as the amplitude of $\omega(\theta)$ at $\theta = 1'$.]

TABLE 5
DIFFERENTIAL V-BAND COUNTS (N deg^{-2} mag^{-1})

Magnitude	$\log_{10}(N)$	σ_{high}	σ_{low}
17.5.....	1.667	0.178	0.306
18.0.....	1.807	0.138	0.204
18.5.....	2.037	0.240	0.580
19.0.....	2.309	0.083	0.103
19.5.....	2.606	0.108	0.144
20.0.....	2.843	0.097	0.125
20.5.....	3.035	0.095	0.122
21.0.....	3.255	0.065	0.077
21.5.....	3.422	0.057	0.066
22.0.....	3.644	0.049	0.055
22.5.....	3.849	0.037	0.040
23.0.....	4.059	0.035	0.038
23.5.....	4.298	0.027	0.029
24.0.....	4.521	0.031	0.034
24.5.....	4.701	0.030	0.032
25.0.....	4.796	0.040	0.044

For each of our pointings, the IC correction, C, was found to be $\sim 0.162 A_\omega$, varying slightly depending on the field geometry and detection mask. The values of C determined for each of the six pointings were comparable since the field sizes and geometries were very similar. Note that the correction becomes important only when measuring the correlation function for galaxies at large separation; for the fields of view analyzed here, the correction has a very small effect on A_ω.

To calculate an error estimate we utilize the fact that we have six separate pointings and compute the uncertainties from the field-to-field variations at each separation. This method of determining the uncertainties is superior to most other analyses which are limited to one or two pointings. These are forced to employ bootstrap resampling techniques in order to estimate uncertainties. However, in this analysis, correlations between measurements on different scales are not taken into consideration, which may result in an underestimate of the χ^2.

Figure 5 shows the two-point angular correlation function for four I-band slices, each 1 mag wide, in the range $20.0 < I \leq 24.0$. We calculated $\omega(\theta)$ using logarithmically spaced bins of width $\Delta \log \theta = 0.2$. On small scales [$\log_{10}(\theta) < 0.2$, $\theta < 1\farcm58$] we estimated the two-point function (eq. [2]) directly from pair counts. On larger scales, $\omega(\theta)$ was determined from counts in cells. The four lines in Figure 5 show the best fit to the data in the range $-1 < \log_{10}(\theta) < 1$ ($6'' < \theta < 10'$), assuming $\delta = 0.8$. (We also fitted A_ω and the slope δ separately, both with and without an IC correction, and found $\delta = 0.8$ to be a good fit to the correlation function for each of the four magnitude intervals.) The best-fit value of $\log_{10} A_\omega$, the logarithm of the amplitude of $\omega(\theta)$ at $1'$, as a function of median I magnitude is shown in Table 6. We find a monotonic decline in A_ω with increasingly faint median I magnitude.

TABLE 6

THE DEPENDENCE OF $A_\omega(1')$ ON MEDIAN MAGNITUDE

Range	Median	$N_{\rm gal}$	$\log_{10} A_\omega(1')$
$20.0 < I \leq 21.0$	20.60	5,235	-1.21 ± 0.08
$21.0 < I \leq 22.0$	21.60	11,535	-1.49 ± 0.04
$22.0 < I \leq 23.0$	22.59	23,842	-1.80 ± 0.04
$23.0 < I \leq 24.0$	23.57	47,141	-2.19 ± 0.07
$21.0 < V \leq 22.0$	21.62	2,598	-1.13 ± 0.06
$22.0 < V \leq 23.0$	22.61	6,883	-1.30 ± 0.05
$23.0 < V \leq 24.0$	23.63	19,411	-1.72 ± 0.05
$24.0 < V \leq 25.0$	24.58	47,057	-2.26 ± 0.09

Figure 6 shows our measurements of $\omega(\theta)$, but for the V band, for four 1 mag wide slices in the range $21.0 < V \leq 25.0$. As with the I band, we find a monotonic decline in the amplitude of the two-point correlation function with increasingly faint V magnitude. The best-fit values of $\log_{10} A_\omega$ as a function of median V magnitude may also be found in Table 6.

Figure 7 compares our measured values of clustering amplitude at $1'$ (as a function of median Cousins I magnitude) with the values obtained by other groups. We compare with the results of Efstathiou et al. (1991); Lidman & Peterson (1996), Woods & Fahlman (1997), Brainerd & Smail (1998), Postman et al. (1998), Cabanac et al. (2000), and McCracken et al. (2000, 2001). At bright magnitudes ($I < 20$) there is good agreement among the measured values of A_ω. However, at fainter magnitudes some discrepancies appear. Our measurements are in very good agreement with those of Efstathiou et al. (1991, using the value quoted in Lidman & Peterson's Table 6) and McCracken et al. (2000, 2001). The clustering amplitude we measure is stronger than that found by Lidman & Peterson. We measure a

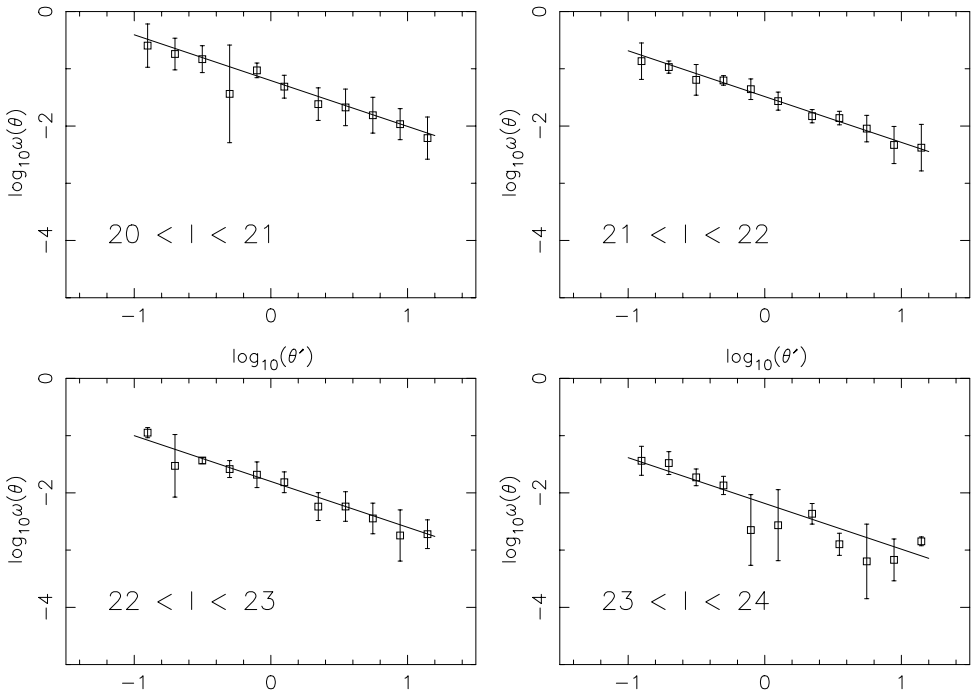

FIG. 5.—Logarithm of the angular correlation function, $\omega(\theta)$, as a function of the logarithm of the angular separation in arcminutes for various I-band slices as shown. The uncertainties are calculated from the pointing-to-pointing variations. The lines show the best fits (Table 6) in the range $-1 < \log_{10}(\theta) < 1 (6'' < \theta < 10')$ assuming a power-law slope of -0.8 for $\omega(\theta)$.

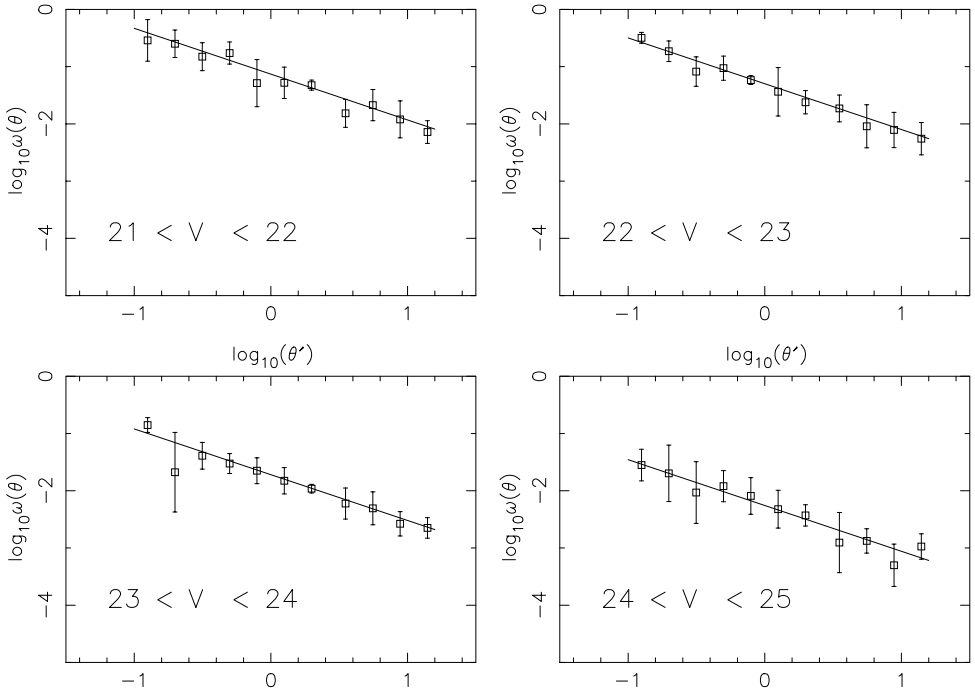

FIG. 6.—Same as Fig. 5, but for the V passband

somewhat lower clustering amplitude than Woods & Fahlman and Cabanac et al. We measure a significantly lower clustering amplitude than Brainerd & Smail and Postman et al.

The discrepancy between our results and those of Woods & Fahlman (1997) and Brainerd & Smail (1998) may be explained by the relatively small area investigated by those studies and the corresponding inherently large uncertainties. Woods & Fahlman had field sizes of 3×49 arcmin^2 and IC correction $\sim$0.02. The corresponding values for Brainerd & Smail were 2×30 arcmin^2 and IC $\sim$0.02. Cabanac et al. report large uncertainties in their photometric zero points, which increase at fainter magnitudes. Any variations in effective depth due to zero-point errors or variations in observing condition (e.g., variations in the seeing) between exposures would artificially mimic large-scale power. The discrepancy with the results of the survey of Postman et al. is more puzzling. The large survey of Postman et al. consisted of 16 deg^2 (256×16 arcmin^2, IC ~ 0.002). They find a shallower best-fit slope to the correlation function ($\delta \simeq 0.7$) for $I > 22$. This disagreement notwithstanding, it seems likely that zero-point variations from frame to frame may remain in the Postman survey.

Figure 8 compares our measured values of clustering amplitude at $1'$ in the V band with the values obtained by Woods & Fahlman (1997) (the only other measurements of A_ω published in this passband). The uncertainties associated with the Woods & Fahlman measurements are larger than for our measurements, but the agreement is generally good

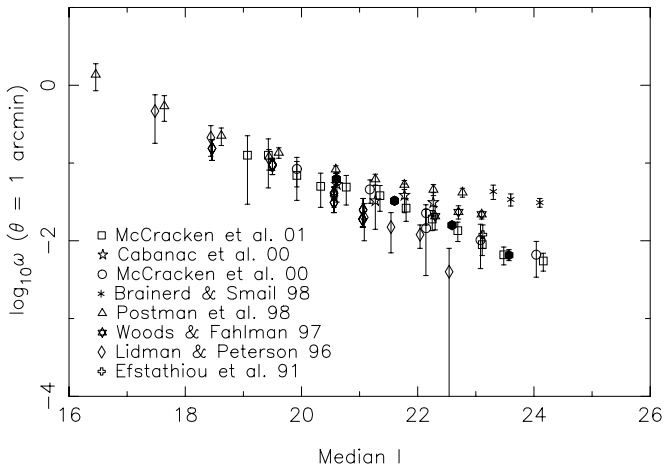

FIG. 7.—Logarithm of the amplitude of the angular correlation function $\omega(\theta)$ at $1'$ for the I passband plotted as a function of median magnitude (see Table 6). The filled hexagons represent our data. Also shown are the measurements from other groups.

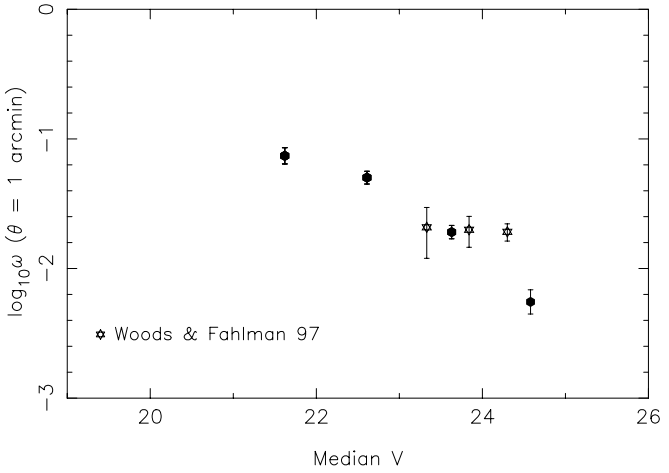

FIG. 8.—Same as Fig. 7, but for the V passband

at $V < 24$. We measure a significantly (factor of 2) lower clustering amplitude than the Woods & Fahlman faintest determination (at $V = 24.3$).

In the next section we predict the correlation function amplitude that we would expect to measure as a function of apparent magnitude, based on deep spectroscopic observations. We then compare these predictions to our measurements. We investigate whether our observations can be matched to the predictions assuming simple analytic models for galaxy clustering evolution.

4.2. *Clustering Strength Predictions*

As mentioned in § 1 the two-point spatial correlation function, $\xi(r)$, for local, optically selected galaxies has been shown to be well described by a power law

$$\xi(r) = (r/r_0)^{-\gamma} , \tag{5}$$

where r is physical (proper) separation and r_0 is the correlation length at $z = 0$. Robust determinations for the power-law slope of $\gamma \simeq 1.8$ and physical correlation length of $r_0 \simeq 5.0\ h^{-1}$ Mpc have been made by many groups (Davis & Peebles 1983; Loveday et al. 1995; Postman et al. 1998; Willmer et al. 1998; Carlberg et al. 2000; Norberg et al. 2001).

Groth & Peebles (1977) proposed the "ϵ-model" to describe the evolution with redshift of the correlation function, measured in terms of proper separation:

$$\xi(r, z) = \left(\frac{r}{r_0}\right)^{-\gamma} (1 + z)^{-(3+\epsilon)} . \tag{6}$$

There are several noteworthy values of the evolutionary parameter ϵ. The clustering pattern is fixed in comoving coordinates if $\epsilon = -1.2$ ($\epsilon = \gamma - 3$): galaxy clusters expand with the universe and clustering does not grow with time. If $\epsilon = 0.0$, "stable clustering," then clustering is fixed in proper coordinates. In this case, the galaxies are dynamically bound and stable at small scales. The clustering grows in this case because the background density of galaxies is diluted by the expansion: it is effectively the voids that are growing. Linear theory predicts $\epsilon = 0.8$ to describe the evolution in the clustering pattern of *dark matter* in an $\Omega_m = 1$ universe (Baugh et al. 1999) (See also, e.g., Colin et al. [1997], Carlberg et al. [2000] and Kauffmann et al. [1999] for ϵ predictions for the dark matter evolution in alternative cosmologies.) If $\epsilon > 0$ then clustering grows with time in proper coordinates, as expected from gravitational collapse.

The relation then (for small angles) between the two-point angular and spatial coordinates, $\omega(\theta)$ and $\xi(r, z)$ is given by Limber's equation (Limber 1953; Peebles 1980):

$$\omega(\theta) = \frac{\Gamma(1/2)\Gamma[(\gamma - 1)/2]}{\Gamma[(\gamma/2)]} \frac{A}{\theta^{\gamma-1}} r_0^{\gamma} , \tag{7}$$

where the Gamma function factor equals 3.68 for $\gamma = 1.8$; A, the amplitude factor, is given by

$$A = \frac{\int_0^{\infty} g(z)[dN(z)/dz]^2\, dz}{\left\{\int_0^{\infty} [dN(z)/dz]\, dz\right\}^2} . \tag{8}$$

Here dN/dz is the number of galaxies per unit redshift interval. The function $g(z)$ depends only on γ, ϵ, and the cosmology,

$$g(z) = \left(\frac{dz}{dx}\right) x^{1-\gamma} F(x) (1 + z)^{-(3+\epsilon-\gamma)}; \tag{9}$$

F gives the correction for curvature,

$$F(x)^2 = 1 + \Omega_k \left(\frac{H_0 x}{c}\right)^2 , \tag{10}$$

and x is the comoving distance at redshift z,

$$x = \frac{c}{H_0} \int_0^z \frac{1}{E(z)}; \tag{11}$$

E is given by

$$E = \left[\Omega_m (1 + z)^3 + \Omega_k (1 + z)^2 + \Omega_{\lambda}\right]^{1/2} , \tag{12}$$

and Ω_k (the "curvature of space") is defined by $\Omega_m + \Omega_{\lambda} + \Omega_k = 1$ (Carroll, Press, & Turner 1992; Hogg 1999; Brown et al. 2000).

Therefore, predictions of galaxy clustering strength, $\omega(\theta)$, are dependent on a number of factors. Namely, these are γ, r_0, ϵ, the assumed redshift distribution $N(z)$, the Hubble constant H_0, and one's choice of cosmology. If the spatial two-point correlation function is well described by a power law (eq. [5]), then the angular two-point correlation function will also be well described by a power law of slope $\delta = \gamma - 1$ (eq. [7]). The physical correlation length at $z = 0$, r_0 (to the power γ), determines the normalization of $\omega(\theta)$. In making our predictions we adopt a local correlation length of $r_0 = 4.9\ h^{-1}$ Mpc, the best-fit real space r_0 determined by the 2dFGRS (Norberg et al. 2001).

Accurate predictions of the correlation amplitude at each magnitude depend crucially on the assumed redshift distribution. [Note that $\omega(\theta)$ decreases with increasing apparent magnitude because of the increasing probability of chance projected alignments of galaxies at very different redshifts.] The value of $\omega(\theta)$ is extremely sensitive to the shape of the assumed redshift distribution, but not to its normalization. As in Wilson et al. (2001a), in making our predictions, we adopt redshift distributions appropriate to each magnitude interval based on spectra from the SSA22 field sample of Cowie (Cowie et al. 1994, 1996; Cowie, Songaila, & Barger 1999; Wilson et al. 2002). We model the normalized redshift distribution as

$$p(z) = 0.5 z^2 \exp(-z/z_0)/z_0^3 , \tag{13}$$

for which the mean redshift is $\overline{z} = 3z_0$ and the median redshift is $z_{\rm median} = 2.67 z_0$. Note that equation (13) has only one free parameter, the redshift scale parameter z_0.

We calculate z_0 (in half-magnitude intervals) by setting the mean redshift to match that from the Cowie sample (allowing for varying numbers of galaxies in each magnitude interval). The Cowie sample reaches a limiting magnitude of $I \simeq 23.5$, $V \simeq 24.5$. At the faintest magnitudes the sample becomes about 20% incomplete. It is thought that the galaxies for which a redshift cannot be determined lie predominantly around $z = 1.5$–2.0. We therefore calculate z_0 in two ways. First we utilize only galaxies in the Cowie sample with secure redshifts, our "raw" model. Second, we assign a redshift of 1.8 to the galaxies from the Cowie catalog without secure redshifts, our "corrected" model. This

TABLE 7
BEST-FIT REDSHIFT SCALE PARAMETER z_0 AS A FUNCTION OF MAGNITUDE

Range	Raw	Corrected
$20.0 < I \leq 20.5$	0.15	0.15
$20.5 < I \leq 21.0$	0.20	0.20
$21.0 < I \leq 21.5$	0.21	0.22
$21.5 < I \leq 22.0$	0.22	0.26
$22.0 < I \leq 22.5$	0.26	0.36
$22.5 < I \leq 23.0$	0.30	0.41
$23.0 < I \leq 23.5$	0.34	0.43
$21.5 < V \leq 22.0$	0.13	0.13
$22.0 < V \leq 22.5$	0.15	0.15
$22.5 < V \leq 23.0$	0.17	0.17
$23.0 < V \leq 23.5$	0.20	0.20
$23.4 < V \leq 24.0$	0.24	0.26
$24.0 < V \leq 24.5$	0.30	0.37

increases the value of the redshift scale parameter z_0 that we employ only at the faintest magnitudes where incompleteness becomes important. It is likely that the true redshift distribution lies between these two extremes. The value of z_0 we adopt to describe the redshift distribution in each half-magnitude interval is shown in Table 7.

In making these predictions of A_ω, we assume a flat lambda ($\Omega_{m0} = 0.3, \Omega_{\lambda 0} = 0.7$) cosmology with $H_0 = 100\ h$ km s^{-1} Mpc^{-1}. The predictions are rather insensitive to the choice of cosmology, because the majority of galaxies lie at relatively low redshift, especially at bright magnitudes. Adopting an Einstein–de Sitter cosmology would decrease the predictions by about 0.2 in the log at the faint end.

The upper panel of Figure 9 shows the *I*-band clustering amplitudes from Figure 7 (for clarity we do not plot the values obtained by other groups). Also shown are the predictions for A_ω assuming redshift distributions based on the Cowie sample and also assuming an evolutionary parameter of either $\epsilon = -1.2$ (*solid line*), 0.0 (*dashed line*), 1.0 (*dot-dashed line*), or 2.0 (*dotted line*). The upper line in each case shows the predictions assuming the raw redshift distribution, the lower line the incompleteness-corrected distribution. Clearly, equation (6) does not provide a very satisfactory fit to the data for any value of ϵ, assuming a smooth extrapolation of the clustering evolutionary model out to this study's fainter magnitude limits. We find that a clustering pattern fixed in physical coordinates, $\epsilon = 0$, provides a reasonable fit to the data at the bright end but that the data fall below the predictions at the faint end.

The lower panel of Figure 9 shows the predictions for A_ω for our *V*-band data (see Table 6 for measured values of A_ω and Table 7 for the z_0 adopted to describe the redshift distribution of each magnitude interval). As for the *I* band, we conclude that equation (6) does not provide a very satisfactory fit to the data for any value of ϵ (assuming a smooth extrapolation of the clustering evolutionary model out to this study's fainter magnitude limits).

In calculating the predicted correlation amplitude we utilized a correlation length of $r_0 = 4.9\ h^{-1}$ Mpc as measured by the 2dFGRS. Adopting a larger or smaller local correlation length would shift the predictions vertically upward or downward.

We conclude that equation (6) does not provide a good fit to the observed evolution in clustering amplitude with redshift. This conclusion was also reached by McCracken et al.

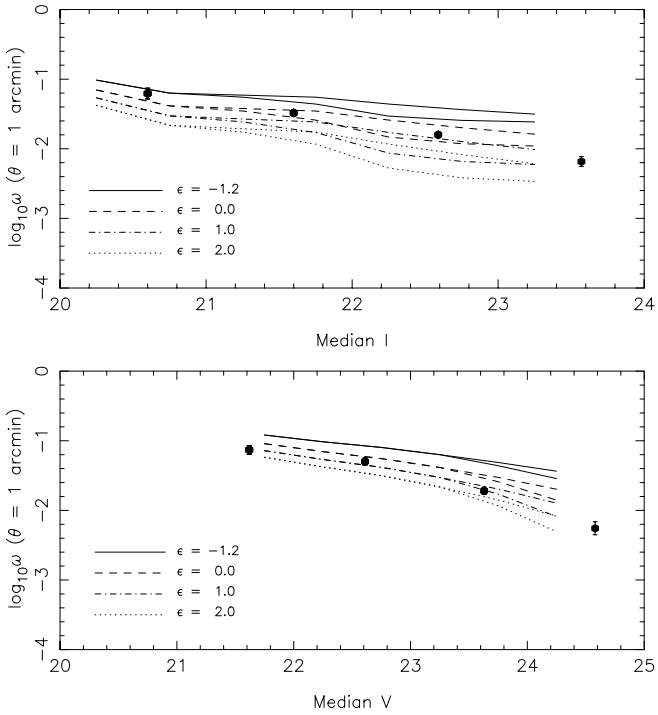

FIG. 9.—Upper panel shows data (*filled hexagons*) as in Fig. 7 for the *I* band. The lines show our predictions assuming redshift distributions based on deep spectroscopic observations, correlation length $r_0 = 4.9\ h^{-1}$ Mpc as measured by the 2dFGRS, and evolutionary parameter $\epsilon = -1.2$ (*solid line*), 0.0 (*dashed line*), 1.0 (*dot-dashed line*), and 2.0 (*dotted line*). Clearly, eq. (6) does not provide a satisfactory fit to the data for any value of ϵ. The lower panel shows same, but for the *V*-band data as in Fig. 8 (see Table 6 for values).

(2001). We interpret the failure of the predictions to match the data as being due to the assumptions of the model being overly simplistic. Equation (6) implicitly assumes that galaxies with different morphologies have similar intrinsic clustering properties. This is known not to be the case locally. Davis & Geller (1976), Giovanelli, Haynes, & Chincarini (1986), Maurogordato & Lachieze-Rey (1991), Iovino et al. (1993), Loveday et al. (1995), Hermit et al. (1996), Guzzo et al. (1997), Willmer et al. (1998), and Norberg et al. (2002) have found early-type galaxies to cluster more strongly than late types. The morphological mix of galaxies in any sample will vary with apparent magnitude due to different *K*-corrections for early- and late-type systems. As one probes fainter in apparent magnitude, a higher preponderance of late types enter the sample (Magliocchetti et al. 2000). Moreover, by selecting on increasingly faint apparent magnitude one samples intrinsically fainter and likely more weakly clustered galaxies (McCracken et al. 2001).

We further investigate the bivariate dependence of galaxy clustering evolution on luminosity and morphology in the remainder of this paper. In the next section we investigate $\omega(\theta)$ as a function of $V-I$ color.

4.3. *The Dependence of $\omega(\theta)$ on $V-I$ Color*

In this section we investigate the dependence of clustering strength on galaxy $V-I$ color. We employ the same catalogs as used in Wilson et al. (2001a), containing galaxies which have been detected in *both I* and *V* images above a threshold significance of 4ν (to ensure that any given "detection" is

TABLE 8
DEPENDENCE OF $A_\omega(1')$ ON $V-I$ COLOR FOR GALAXIES IN THE RANGE $20.0 < I \leq 23.0$

Color Range	N_{gal}	$\log_{10} A_\omega(1')$
$0.0 < V-I \leq 0.5$.....	136	0.06 ± 0.45
$0.5 < V-I \leq 1.0$.....	4,209	-1.27 ± 0.08
$1.0 < V-I \leq 1.5$.....	13,511	-1.64 ± 0.08
$1.5 < V-I \leq 2.0$.....	13,587	-1.50 ± 0.04
$2.0 < V-I \leq 2.5$.....	5,757	-1.20 ± 0.08
$2.5 < V-I \leq 3.0$.....	4,211	-1.03 ± 0.12
$3.0 < V-I \leq 3.5$.....	1,833	-0.78 ± 0.08

truly a real object). Galaxies tend to be detected at higher significance in the I-band images. We subdivided the data into seven intervals with $V-I$ color ranging from 0.0 to 3.5 and $\Delta(V-I) = 0.5$ (Table 8 shows the number of galaxies in each color interval). As in § 4.1, we again assume that $\omega(\theta)$ is well described by a power law of slope $\delta = 0.8$, and we fit over the range $-1.0 < \log_{10} \omega(\theta) \leq 1.0$.

Figure 10 shows clustering amplitude as a function of color for galaxies in the range $20.0 < I \leq 23.0$. Figure 2 shows a turnover in the V-band counts at $V \simeq 25$, and thus we may be subject to missing fainter galaxies from the redder ($V-I > 2$) intervals. Table 8 shows the best-fit values of A_ω obtained for each color interval. As in § 4.1, the uncertainties were estimated from the field-to-field variations between our six pointings. The dashed line in Figure 10 shows the correlation amplitude (-1.80 for a median I magnitude of 22.59) obtained for the full field sample in § 4.1 (Table 6).

As seen from Figure 10, red galaxies ($V-I \simeq 3$) have a clustering amplitude about 10 times larger than that measured for the full sample in § 4.1. As we shall discuss further in § 4.4, galaxies with color $V-I = 3$ are exclusively early types occupying a narrow range in redshift at about $z = 1$. Since the redshift distribution $N(z)$ for these red galaxies is rather narrow, chance alignments of galaxies of the same color at significantly higher or lower redshift cannot occur and hence the measured angular correlation function is not diluted as it is for galaxies with colors in the range $1 < (V-I) < 2$, which are more widely distributed in redshift. The high clustering amplitude found for extremely red galaxies is also due in small part to these being of a morphological type that (at least locally) clusters more strongly than later types.

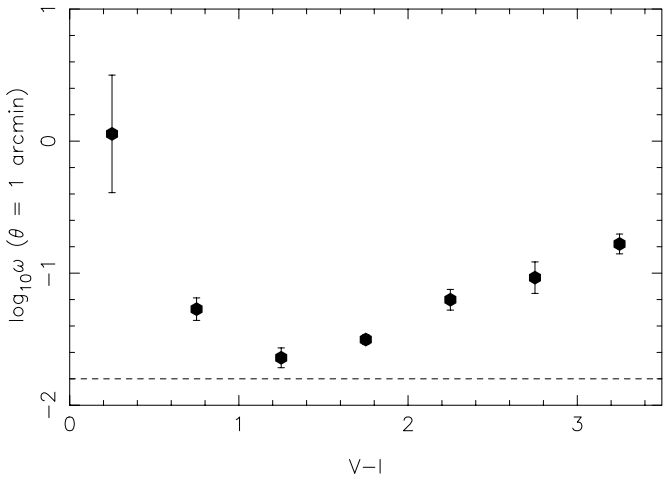

FIG. 10.—Logarithm of the amplitude of the angular correlation function $\omega(\theta)$ at 1′ as a function of $V-I$ color for galaxies in the magnitude range $20 < I \leq 23$ (see Table 8). Extremely red and extremely blue galaxies are seen to cluster more strongly than those of intermediate color. The dashed line shows the amplitude measured in § 4.1 for the full field sample with median I magnitude of 22.59. In all cases, the clustering amplitude is higher than for the full field population.

As noted by McCracken et al. (2001), we also find an upturn in the clustering amplitude of extremely blue galaxies ($V-I \simeq 0.5$). A similar effect was noted by Landy et al. (1996). The most likely explanation for the strong angular clustering amplitude found for the blue galaxies is that these galaxies are all situated at relatively low redshifts. As with the red sample, the redshift distribution $N(z)$ of these extremely blue galaxies is rather narrow and thus A_ω is not diluted as strongly in projection over redshift as is the intermediate sample.

The results of this section and of § 4.2 strongly suggest that studying and interpreting galaxy clustering as a function either of median magnitude or of color is greatly complicated by the varying morphologies and intrinsic luminosities of galaxies contained in the different samples. A far more promising approach would be to isolate the same population and study its clustering evolution with redshift. Given fluxes in only two passbands, as we have here, it is impossible to select and measure evolution in $\omega(\theta)$ for all morphological types. However, as we show in the next section, it is possible to use crude photometric redshift determinations to isolate and analyze the clustering evolution of $L*$ early-type galaxies with redshift.

4.4. *The Dependence of $\omega(\theta)$ on Morphological Type*

As in Wilson et al. (2001a), we use $V-I$ color combined with an I-band magnitude cut to select a sample of bright early-type galaxies. This technique depends on the fact that early-type galaxies are the reddest galaxies at any given redshift. By selecting galaxies of some color, we see a superposition of early types at redshift z_E such that $c = c_E(z_E)$ and later types at their appropriate, but considerably higher, redshift. An $L \sim L*$ early-type galaxy appears much brighter than an $L \sim L*$ spiral galaxy, and as explained in more detail in § 2.2 of Wilson et al., with a judicious cut in I magnitude it is possible to isolate a bright early-type galaxy sample.

We divide the data into nine ($\Delta z = 0.1$) bins (the lowest redshift $z = 0.1 \pm 0.05$ bin contains very few galaxies so is discarded here). In addition to a morphological dependence, there has recently been quite considerable evidence in the literature for a luminosity dependence: luminous galaxies clustering more strongly than their fainter counterparts. Such a luminosity dependence has been reported by Benoist et al. (1996), Guzzo et al. (1997), Willmer et al. (1998), Small et al. (1999), Norberg et al. (2001), Firth et al. (2002), and Zehavi et al. (2002). The evidence for a dramatic increase in clustering strength with increasing luminosity for $L > L*$ galaxies is the most compelling. Indeed, Norberg et al. (2002) find a factor of 2.5 difference between the clustering strength of $L*$ and $4L*$ galaxies and suggest that it is in fact luminosity, not type, that is the dominant factor (Norberg et al. measure a clustering strength for early types about 50% higher than that for late types at all luminosities).

TABLE 9
$A_\omega(1')$ FOR EARLY-TYPE GALAXIES AS A FUNCTION OF REDSHIFT

Redshift	$N_{\rm gal}$	$\log_{10} A_\omega(1')$
0.2 ± 0.05...	136	0.05 ± 0.36
0.3 ± 0.05...	366	-0.21 ± 0.07
0.4 ± 0.05...	569	-0.54 ± 0.11
0.5 ± 0.05...	559	-0.53 ± 0.15
0.6 ± 0.05...	389	-0.60 ± 0.26
0.7 ± 0.05...	551	-0.38 ± 0.10
0.8 ± 0.05...	575	-0.47 ± 0.16
0.9 ± 0.05...	237	-0.28 ± 0.12

In an effort to eliminate any complicating effect of a luminosity-dependent component to $\omega(\theta)$, we decided to make a further restrictive cut to the early-type galaxies we allowed into our sample at each redshift. We chose to exclude all galaxies with absolute magnitude fainter than $M = M_* + 1$ from our analysis. This ensures that the remaining sample has an effective luminosity $L_{\rm eff} \sim L_*$ ($L_{\rm eff} = 0.98L_*$ if one assumes the 2dFGRS value of $L_* = -19.61$ (Folkes et al. 1999; see also Madgwick et al. 2002). This assumes that L_* for early-type galaxies does not evolve between $z = 0$ and 1. Based on our knowledge about early-type evolution with redshift this does not seem a grossly inaccurate assumption, e.g., Lilly et al. (1995) found that the red (redder than present-day Sbc and hence early type) sample from the Canada-France Redshift Survey, was consistent with no change in L_* between $z \sim 0.8$ and $z \sim 0.3$ (their red sample was also consistent with a change of *at most* a few tenths of a magnitude).

Table 9 shows the number of galaxies in each redshift interval that meet our criteria. In estimating A_ω, we once more assumed that $\omega(\theta)$ was well described by a power law with slope $\delta = 0.8$ ($= \gamma - 1$). Slightly steeper slopes have been claimed for the spatial correlation function slope γ for early-type galaxies, i.e., 1.87 ± 0.07 (Loveday et al. 1995), 2.05 ± 0.1 (Guzzo et al. 1997), 1.91 ± 0.06 (Willmer et al. 1998), 1.91 ± 0.06 (Shepherd et al. 2001), and 1.87 ± 0.09 (Norberg et al. 2002). A slightly steeper slope would have negligible effect on our conclusions and is far from being the main source of uncertainty. Note also that by measuring the correlation function amplitude at a fixed angular scale of $1'$ we are measuring at increasing projected radius with redshift, ranging from about 140 h^{-1} kpc at $z = 0.2$ to about 330 h^{-1} kpc at $z = 0.9$. This analysis, therefore, assumes that any bias is not a function of scale (Magliocchetti et al. 2000).

Figure 11 shows the logarithm of A_ω, the amplitude of $\omega(\theta)$ at $1'$, as a function of redshift for early types. The measured values of the two-point correlation function amplitude at each redshift may be found in Table 9. For comparison, superimposed on Figure 11 are the predictions assuming a correlation length of $r_0 = 5.7\ h^{-1}$ Mpc, the value determined by the 2dFGRS for local early types with $L = L_* \pm 0.5$ (Norberg et al. 2002, their Table 2). The various lines indicate the predictions assuming evolutionary parameter $\epsilon = -1.2$ (*solid line*), 0.0 (*dashed line*), 1.0 (*dot-dashed line*), or 2.0 (*dotted line*). The resulting predictions assuming the 2dFGRS value of r_0 match our measurements of the clustering amplitude reasonably well over the whole range of redshift. Clustering fixed in comoving coordinates,

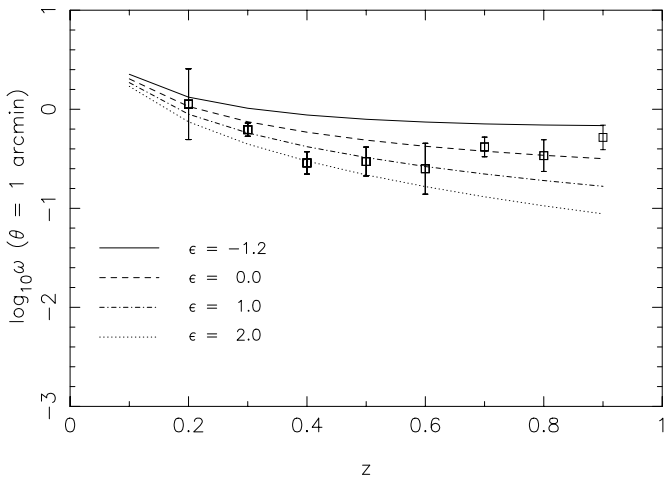

FIG. 11.—Logarithm of the amplitude of the angular correlation function $\omega(\theta)$ at $1'$ for L_* early-type galaxies as a function of redshift. The lines show predictions for evolutionary parameter $\epsilon = -1.2$ (*solid line*), 0.0 (*dashed line*), 1.0 (*dot-dashed line*), and 2.0 (*dotted line*), assuming $r_0 = 5.7\ h^{-1}$ Mpc, the correlation length of early-type galaxies determined locally by the 2dFGRS.

$\epsilon = -1.2$, appears somewhat to overestimate the measured clustering amplitude. At the other extreme, rapid growth in clustering with time, $\epsilon = 2.0$, appears rather to underestimate the actual data.

Figure 12 shows the same data as Figure 11 but plotted on a log-log scale. Here we assume a correlation function slope of $\gamma = 1.8$ and a flat lambda cosmology as before. In this case, however, at each redshift we subtract the Gamma function and cosmological components of the two-point function (eqs. [7] and [9]) from our measured value of A_ω. The remaining r_0- and ϵ-dependent portion of the correlation function amplitude $[\gamma \log r_0 - (3 + \epsilon - \gamma)\log(1 + z)]$ at each redshift is then plotted. The redshift baseline is too small and the uncertainties too large to solve meaningfully

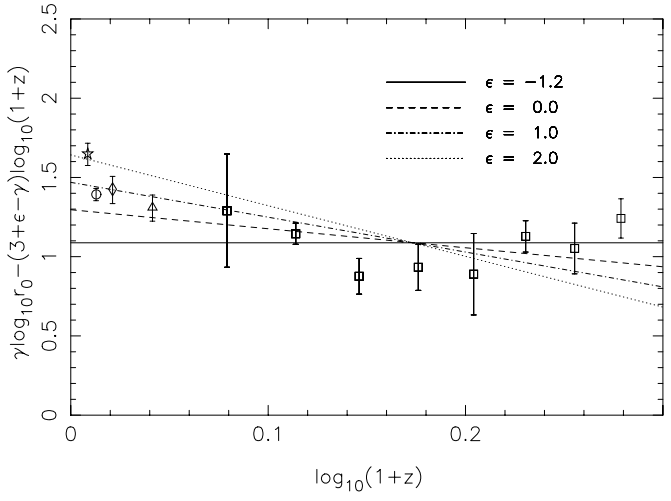

FIG. 12.—Logarithm of the cosmology-independent component of the angular correlation function $\omega(\theta)$ at $1'$ for L_* early-type galaxies assuming $\gamma = 1.8$. The lines show best-fit physical correlation length r_0, for evolutionary parameters $\epsilon = -1.2$ (*solid line*), 0.0 (*dashed line*), 1.0 (*dot-dashed line*), or 2.0 (*dotted line*). Also shown are the values measured by Loveday et al. (*diamond*), Guzzo et al. (*star*), Willmer et al. (*circle*), and Norberg et al. (*triangle*).

TABLE 10
Best-Fit Physical Correlation Length r_0 and Reduced χ^2 for Various Values of Evolutionary Parameter ϵ

ϵ	r_0	χ^2/dof
−1.2.....	4.02 ± 0.22	1.01
0.0.....	5.25 ± 0.29	1.59
1.0.....	6.55 ± 0.36	2.70
2.0.....	8.17 ± 0.45	4.40

for r_0 and ϵ simultaneously. We therefore solved solely for r_0. The best-fit physical clustering length $r_0(\epsilon)$ was found to be 4.02 ± 0.22 (−1.2), 5.25 ± 0.28 (0.0), 6.55 ± 0.36 (1.0), and 8.17 ± 0.45 (2.0), as shown in Table 10. The lines superimposed onto Figure 12 show these best-fit estimates (*solid line:* $\epsilon = -1.2$; *dashed line:* $\epsilon = 0$; *dot-dashed line:* $\epsilon = 1$; *dotted line:* $\epsilon = 2$).

Stronger constraints may be placed on the evolutionary parameter ϵ if we consider our data in conjunction with local measurements. The Norberg et al. measurement of 5.7 ± 0.6 ($M_* - 0.5 < M < M_* + 0.5$) is that which most closely resembles our own study with regard to the range of absolute luminosity of galaxies included in the sample ($M_* - 0.5 < M < M_* + 0.5$; cf. $M < M_* + 1.0$ in this analysis). However, we also now compare with the clustering length measured locally by other groups for early-type galaxies (the values in parentheses show the range in absolute magnitude). Shepherd et al. (2001) obtained 5.45 ± 0.28 ($M < M_* - 1.0$) from the CNOC2 survey. However, other groups have obtained slightly larger correlation lengths. Loveday et al. (1995) measured 6.4 ± 0.7 ($M_* - 0.5 < M < M_* + 0.5$) for the Stromlo-APM survey, Willmer et al. (1998) measured 6.06 ± 0.39 ($M < M_* + 5.5$) for the SSRS2 survey, and Guzzo et al. (1997) measured 8.35 ± 0.75 for the Perseus-Pisces survey. Note that the latter (Guzzo et al.) result is for a survey known to contain a high abundance of local clusters and therefore the high correlation length is unsurprising. Also plotted onto Figure 12 are the values measured by Loveday et al. (*diamond*), Guzzo et al. (*star*), Willmer et al. (*circle*), and Norberg et al. (*triangle*). Even with the above-mentioned caveats, it would appear from Figure 12 that in order to match the "local" value for early-type galaxies, the correlation length of such galaxies would be required to grow with time ($\epsilon \gtrsim 0.0$).

Equation (6) is a purely empirical model and is not necessarily expected to be valid at all redshifts. In particular, this model predicts monotonic evolution in r_0 with redshift, which is at odds with predictions (although these provide rather weak constraints at present) from N-body simulations. For example, from their semianalytic model, Baugh et al. (1999, their Fig. 2) suggest that $\epsilon = 0$ is a good descriptor of the behavior of the galaxy correlation function between $z = 0$ and $z = 1$, i.e., clustering does not evolve in physical coordinates and there is a monotonic decrease in the physical correlation length with look-back time during that epoch. However, between $z = 1$ and $z = 2$, a minimum in the correlation length is reached. At higher redshift, Baugh et al. predict an upturn in the correlation length, and thus equation (6) would not describe galaxy clustering well in the higher redshift regime. Similar conclusions were reached from simulations by Kauffmann et al. (1999). Such predictions of an upturn in the correlation length at higher redshift are supported by the $z \sim 3$ measurements of Lyman-break galaxies (Adelberger et al. 1998; Giavalisco et al. 1998). Thus, while the ϵ model does appear to be in qualitative agreement with our measurements of early type clustering at $z < 1$, any evolution in clustering at higher redshift may well be poorly described by the ϵ formalism. For now, based on our measurements, the predictions from semianalytic modeling, and the requirement to match the clustering lengths measured locally for early-type galaxies, we assume the "null hypothesis," namely, that clustering is fixed in physical coordinates. We conclude, for now at least, that the ϵ model with $\epsilon = 0.0$ and a present-day correlation length $r_0 = 5.25 \pm 0.28$ provides a satisfactory fit to observations over the redshift range $0 < z < 0.9$. (See Hogg, Cohen, & Blandford [2000] for a similar conclusion of minimal evolution relative to stable clustering in the redshift range $0 < z < 1$ although in that case comparing heterogeneous samples of galaxies with respect to absolute magnitude, redshift, morphological type, correlation function slope γ, and cosmology.) Note that for a correlation function of the form $\xi(r) = (r/r_0)^{-\gamma}$, clustering density falls with radius as $r^{-\gamma}$ and the cosmic mean rises with redshift as $(1 + z)^3$, so the stable clustering prediction is for the proper correlation length to decrease with increasing redshift as $r_0(z) = r_0(0)(1 + z)^{-3/\gamma}$.

Interestingly, we note that the clustering strength we measure is significantly weaker than that found for extremely red objects (EROs) at $z > 1$. Daddi et al. (2000, 2001) used K- and R-band imaging, McCarthy et al. (2001) used H- and I-band imaging, and Firth et al. (2002) used R- and H-band imaging all from the Las Campanas Infrared Survey to select EROs (which are thought to be predominantly elliptical galaxies in the redshift range $1 < z < 1.5$). Daddi et al. measured a *comoving* correlation length of $12 \pm 3\ h^{-1}$ Mpc for an effective redshift $z \sim 1.2$. McCarthy et al. measured a slightly smaller *comoving* correlation length of $9.5 \pm 0.5\ h^{-1}$ Mpc. Using our preferred $\epsilon = 0$, these comoving values can be converted to physical correlation lengths via $x_0 = r_0(1 + z)^{-(3+\epsilon-\gamma)/\gamma}$, where $r_0 = x_0(z = 0)$, which translates to $r_0 \sim 12$–$18\ h^{-1}$ Mpc. Even if one assumed that these galaxies underwent no evolution in comoving clustering ($\epsilon = -1.2$, i.e., $x_0 = x_z$), this would result in a present-day correlation length of $r_0 \sim 9$–$12\ h^{-1}$ Mpc. Even allowing for these two samples containing brighter galaxies than ours, it would be very difficult to reconcile such large correlation lengths for the ERO's with our measurements for $0 < z < 1$ early types. Indeed, it would be difficult to reconcile such high values of correlation length with the 8.33 ± 1.82 found locally for the *brightest* interval in the Norberg et al. (2002, their Table 2) sample. Firth et al. measure $r_0 = 7.7 \pm 2.4$ for $\epsilon = -1.2$ or $r_0 = 12.1$ assuming $\epsilon = 0$. It is possible that the width of the redshift distributions $N(z)$ (derived from photometric redshifts) used in the Las Campanas estimates have been overestimated leading to an increase in the estimates of r_0. Alternatively, the larger inferred values of r_0 may be the result of an increasing biasing with redshift (Mo & White 1996). A yet further possibility is that ERO's are not truly field early types but may show stronger clustering strengths because they are cluster elliptical galaxies in the process of forming (Moustakas & Somerville 2002). Further data will be required to resolve this controversy.

5. CONCLUSIONS

We investigated the dependence of the two-point galaxy angular correlation function on median magnitude, $V-I$ color and morphology. We found $\omega(\theta)$ to be consistent with a power law of slope -0.8 for both I and V passbands, down to our faintest limits of $I = 24$ and $V = 25$. We found A_ω, the amplitude of $\omega(\theta)$ at $1'$, to decrease monotonically with increasingly faint median magnitude. We used spectroscopic redshifts measured from Cowie's SSA22 field sample to model the galaxy redshift distribution as a function of apparent magnitude. We compared the measured values of clustering amplitude A_ω with the values predicted in an $\Omega_{m0} = 0.3, \Omega_{\lambda 0} = 0.7$ cosmology. We found that simple redshift-dependent models with evolutionary parameter ϵ were inadequate to describe the evolution of clustering. We concluded that allowance must be made for the increasing proportion of later type and fainter galaxies (with weaker correlation strengths) entering our sample at fainter magnitudes.

We also found a strong clustering dependence on color. Extremely blue galaxies ($V-I \sim 0.5$) were found to have a clustering amplitude about 15–20 times as high as the full field population. This is most likely to be because many of these blue galaxies are situated at very similar relatively low redshift, and therefore $\omega(\theta)$ is minimally diluted by projection effects. Extremely red galaxies ($V-I \sim 3$) were found to have an clustering amplitude about 10 times as high as the full sample. We similarly interpreted the stronger clustering amplitude for redder galaxies to be mainly due to these galaxies occupying a narrow range in redshift at $z = 1$. The stronger signal is also due in part to these being early-type galaxies which locally cluster more strongly than later types.

We then presented the first attempt to investigate redshift evolution utilizing a population of galaxies of the *same* absolute luminosity and morphological type. We used $V-I$ color to isolate a sample of early-type galaxies and investigated the evolution in their clustering. By making an *identical* cut in absolute magnitude to our early-type sample at each redshift, we determined $\omega(\theta)$ for galaxies with effective luminosity $L_{\rm eff} \simeq L_*$ (assuming no evolution in the luminosity function with redshift) in eight redshift intervals spanning $z = 0.2$–0.9. Although uncertainties were large, we found the evolution in the clustering of these galaxies to be consistent with stable clustering ($\epsilon = 0$). We found L_* early-type galaxies to have correlation length $r_0 = 5.25 \pm 0.28\ h^{-1}$ Mpc (assuming $\epsilon = 0$), a slightly higher correlation length than has been found for the local full field population. Our measured value of r_0 is in good agreement with the 2dFGRS measurement of correlation strength for L_* early-type galaxies in the local universe.

Over the last few years it has become increasingly apparent that galaxy clustering has a bivariate dependence on both morphological type and intrinsic luminosity. Clearly, if there are differences between the clustering of various different samples of galaxies we can immediately infer that at least one of the galaxy samples is a biased tracer of the underlying mass distribution. This paper presented the first attempt to separate the relative contributions of luminosity and type and to investigate the evolution in clustering of a single galaxy population. In the future, huge quantities of new data from galaxy redshift and large-area imaging surveys currently in progress will allow galaxy samples to be selected more precisely by luminosity and type. The 2dFGRS and SDSS are in the process of measuring spectroscopic redshifts for millions of galaxies and will determine, with incredible accuracy, the "local" correlation function (both slope and amplitude) as a function of galaxy morphological type and absolute luminosity. Preliminary findings have already been reported by Norberg et al. (2001, 2002), Connolly et al. (2002), Infante et al. (2002), Zehavi et al. (2002), Dodelson et al. (2002), and Tegmark et al. (2002). At higher redshift, next-generation redshift surveys such as DEEP2 (Davis & Faber 1998; Coil, Davis, & Szapudi 2001) or VIRMOS (Le Fèvre et al. 2001) will provide tens of thousands of galaxy redshifts.

In the more immediate future, large multipassband surveys such as the Deep Lens Survey[5] are measuring tens of millions of galaxies over tens of square degrees, which will result in much more accurate photometric redshift determinations than possible in this study. The greater range of absolute luminosity then available (limited here to $M \sim M_* \pm 1$) will allow any luminosity dependence to the early-type galaxy correlation function to be determined more precisely as a function of redshift. Moreover, increased numbers of early-type galaxies will greatly reduce uncertainties in the measurement of the amplitude and slope of the correlation function. Finally, the availability of more than two passbands will also allow photometric redshifts for late-type galaxies to be determined and a similar investigation to be undertaken into their clustering evolution.

We thank Len Cowie for kindly allowing the use of the Hawaii Survey Fields data set. It is a pleasure to thank Håkon Dahle, Ian Dell'Antonio, Nick Kaiser, and Gerry Luppino for many useful discussions. The research described in this paper was carried out, in part, by the Jet Propulsion Laboratory, California Institute of Technology, and was sponsored by the National Aeronautics and Space Administration.

[5] See http://dls.bell-labs.com.

REFERENCES

Adelberger, K. L., Steidel, C. C., Giavalisco, M., Dickinson, M., Pettini, M., & Kellogg, M. 1998, ApJ, 505, 18
Arnouts, S., Cristiani, S., Moscardini, L., Matarrese, S., Lucchin, F., Fontana, A., & Giallongo, E. 1999a, MNRAS, 310, 540
Arnouts, S., D'Odorico, S., Cristiani, S., Zaggia, S., Fontana, A., & Giallongo, E. 1999b, A&A, 341, 641
Bardeen, J. M., Bond, J. R., Kaiser, N., & Szalay, A. S. 1986, ApJ, 304, 15
Baugh, C. M., Benson, A. J., Cole, S., Frenk, C. S., & Lacey, C. G. 1999, MNRAS, 305, L21
Benoist, C., Maurogordato, S., da Costa, L. N., Cappi, A., & Schaeffer, R. 1996, ApJ, 472, 452
Bernstein, G. M., Tyson, J. A., Brown, W. R., & Jarvis, J. F. 1994, ApJ, 426, 516
Brainerd, T. G., & Smail, I. 1998, ApJ, 494, L137
Brainerd, T. G., Smail, I., & Mould, J. 1995, MNRAS, 275, 781
Brown, M. J. I., Webster, R. L., & Boyle, B. J. 2000, MNRAS, 317, 782
Brunner, R. J., Szalay, A. S., & Connolly, A. J. 2000, ApJ, 541, 527
Cabanac, R. A., de Lapparent, V., & Hickson, P. 2000, A&A, 364, 349
Carlberg, R. G., Yee, H. K. C., Morris, S. L., Lin, H., Hall, P. B., Patton, D., Sawicki, M., & Shepherd, C. W. 2000, ApJ, 542, 57
Carroll, S. M., Press, W. H., & Turner, E. L. 1992, ARA&A, 30, 499
Coil, A. L., Davis, M., & Szapudi, I. 2001, PASP, 113, 1312
Colin, P., Carlberg, R. G., & Couchman, H. M. P. 1997, ApJ, 490, 1
Connolly, A. J., Szalay, A. S., & Brunner, R. J. 1998, ApJ, 499, L125
Connolly, A. J., et al. 2002, ApJ, 579, 42
Cowie, L. L., Gardner, J. P., Hu, E. M., Songaila, A., Hodapp, K. W., & Wainscoat, R. J. 1994, ApJ, 434, 114
Cowie, L. L., Songaila, A., & Barger, A. J. 1999, AJ, 118, 603 (CSB)

Cowie, L. L., Songaila, A., Hu, E. M., & Cohen, J. G. 1996, AJ, 112, 839
Daddi, E., Broadhurst, T., Zamorani, G., Cimatti, A., Röttgering, H., & Renzini, A. 2001, A&A, 376, 825
Daddi, E., Cimatti, A., Pozzetti, L., Hoekstra, H., Röttgering, H. J. A., Renzini, A., Zamorani, G., & Mannucci, F. 2000, A&A, 361, 535
Davis, M., & Faber, S. M. 1998, in Wide Field Surveys in Cosmology, ed. S. Colombi & Y. Mellier (Paris: Editions Frontières), 333
Davis, M., & Geller, M. J. 1976, ApJ, 208, 13
Davis, M., & Peebles, P. J. E. 1983, ApJ, 267, 465
Dodelson, S., et al. 2002, ApJ, 572, 140
Driver, S. P., Phillips, S., Davies, J. I., Morgan, I., & Disney, M. J. 1994, MNRAS, 268, 393 (DPDMD)
Efstathiou, G., Bernstein, G., Tyson, J. A., Katz, N., & Guhathakurta, P. 1991, ApJ, 380, L47
Firth, A. E., et al. 2002, MNRAS, 332, 617
Folkes, S., et al. 1999, MNRAS, 308, 459
Fynbo, J. U., Freudling, W., & Möller, P. 2000, A&A, 355, 37
Gardner, J. P., Sharples, R. M., Carrasco, B. E., & Frenk, C. S. 1996, MNRAS, 282, L1
Giavalisco, M., Steidel, C. C., Adelberger, K. L., Dickinson, M. E., Pettini, M., & Kellogg, M. 1998, ApJ, 503, 543
Giovanelli, R., Haynes, M. P., & Chincarini, G. L. 1986, ApJ, 300, 77
Groth, E. J., & Peebles, P. J. E. 1977, ApJ, 217, 385
Guzzo, L., Strauss, M. A., Fisher, K. B., Giovanelli, R., & Haynes, M. P. 1997, ApJ, 489, 37
Guzzo, L., et al. 2000, A&A, 355, 1
Hermit, S., Santiago, B. X., Lahav, O., Strauss, M. A., Davis, M., Dressler, A., & Huchra, J. P. 1996, MNRAS, 283, 709
Hogg, D. 1999, preprint (astro-ph/9905116)
Hogg, D. W., Cohen, J. G., & Blandford, R. 2000, ApJ, 545, 32
Hudon, J. D., & Lilly, S. J. 1996, ApJ, 469, 519
Infante, L., & Pritchet, C. J. 1995, ApJ, 439, 565
Infante, L., et al. 2002, ApJ, 567, 155
Iovino, A., Giovanelli, R., Haynes, M., Chincarini, G., & Guzzo, L. 1993, MNRAS, 265, 21
Kaiser, N. 1984, ApJ, 284, L9
Kaiser, N., Squires, G., & Broadhurst, T. G. 1995, ApJ, 449, 460 (KSB)
Kaiser, N., Wilson, G., & Luppino, G. 2000, preprint (astro-ph/0003338) (KWL)
Kauffmann, G., Colberg, J., M., Diaferio, A., & White, S. D. M. 1999, MNRAS, 307, 529
Landolt, A. U. 1992, AJ, 104, 340
Landy, S. D., & Szalay, A. S. 1993, ApJ, 412, 64
Landy, S. D., Szalay, A. S., & Koo, D. C. 1996, ApJ, 460, 94
Le Fèvre, O., Hudon, D., Lilly, S. J., Crampton, D., Hammer, F., & Tresse, L. 1996, ApJ, 461, 534
Le Fèvre, O., et al. 2001, in Deep Fields, ed. S. Christiani, A. Renzini, & R. E. Williams (Berlin: Springer), 236
Lidman, C. E., & Peterson, B. A. 1996, MNRAS, 279, 1357
Lilly, S. J., Tresse, L., Hammer, F., Crampton, D., & Le Fevre, O. 1995, ApJ, 455, 108
Limber, D. N. 1953, ApJ, 117, 134
Lin, H., Kirshner, R. P., Shectman, S. A., Landy, S. D., Oemler, A., Tucker, D. L., & Schechter, P. L. 1996, ApJ, 471, 617
Loveday, J., Maddox, S. J., Efstathiou, G., & Peterson, B. A. 1995, ApJ, 442, 457
Maddox, S. J., Sutherland, W. J., Efstathiou, G., Loveday, J., & Peterson, B. A. 1990, MNRAS, 247, 1P
Madgwick, D. S., et al. 2002, MNRAS, 333, 133
Magliocchetti, M., Bagla, J. S., Maddox, S. J., & Lahav, O. 2000, MNRAS, 314, 546
Maurogordato, S., & Lachieze-Rey, M. 1991, ApJ, 369, 30
McCarthy, P. J., et al. 2001, ApJ, 560, L131
McCracken, H. J., Le Fèvre, O., Brodwin, M., Foucaud, S., Lilly, S. J., Crampton, D., & Mellier, Y. 2001, A&A, 376, 756
McCracken, H. J., Shanks, T., Metcalfe, N., Fong, R., & Campos, A. 2000, MNRAS, 318, 913
Metcalfe, N., Shanks, T., Campos, A., McCracken, H. J., & Fong, R. 2001, MNRAS, 323, 795
Mo, H. J., & White, S. D. M. 1996, MNRAS, 282, 347
Moustakas, L. A., & Somerville, R. S. 2002, ApJ, 577, 1
Neuschaefer, L. W., & Windhorst, R. A. 1995, ApJ, 439, 14
Norberg, P., et al. 2001, MNRAS, 328, 64
———. 2002, MNRAS, 332, 827
Peebles, P. J. E. 1980, The Large-Scale Structure of the Universe (Princeton: Princeton Univ. Press)
Phillipps, S., Fong, R., Fall, R. S. E. S. M., & MacGillivray, H. T. 1978, MNRAS, 182, 673
Postman, M., Lauer, T. R., Szapudi, I., & Oegerle, W. 1998, ApJ, 506, 33
Roche, N., & Eales, S. A. 1999, MNRAS, 307, 703
Roche, N., Ratnatunga, K., Griffiths, R. E., Im, M., & Neuschaefer, L. 1996, MNRAS, 282, 1247
Roche, N., Shanks, T., Metcalfe, N., & Fong, R. 1993, MNRAS, 263, 360
Schlegel, D. J., Finkbeiner, D. P., & Davis, M. 1998, ApJ, 500, 525
Shanks, T., Fong, R., Ellis, R. S., & MacGillivray, H. T. 1980, MNRAS, 192, 209
Shepherd, C. W., Carlberg, R. G., Yee, H. K. C., & Ellingson, E. 1997, ApJ, 479, 82
Shepherd, C. W., Carlberg, R. G., Yee, H. K. C., Morris, S. L., Lin, H., Sawicki, M., Hall, P. B., & Patton, D. R. 2001, ApJ, 560, 72
Smail, I., Hogg, D. W., Yan, L., & Cohen, J. G. 1995, ApJ, 449, L105
Small, T. A., Ma, C., Sargent, W. L. W., & Hamilton, D. 1999, ApJ, 524, 31
Szapudi, I., & Szalay, A. S. 1998, ApJ, 494, L41
Tegmark, M., et al. 2002, ApJ, 571, 191
Teplitz, H. I., Hill, R. S., Malumuth, E. M., Collins, N. R., Gardner, J. P., Palunas, P., & Woodgate, B. E. 2001, ApJ, 548, 127
Villumsen, J. V., Freudling, W., & da Costa, L. N. 1997, ApJ, 481, 578
Willmer, C. N. A., da Costa, L. N., & Pellegrini, P. S. 1998, AJ, 115, 869
Wilson, G., Cowie, L. L., Barger, A. J., & Burke, D. J. 2002, AJ, 124, 1258
Wilson, G., Kaiser, N., & Luppino, G. A. 2001a, ApJ, 556, 601
Wilson, G., Kaiser, N., Luppino, G. A., & Cowie, L. L. 2001b, ApJ, 555, 572
Woods, D., & Fahlman, G. G. 1997, ApJ, 490, 11
Zehavi, I., et al. 2002, ApJ, 571, 172